

# Cubic boron phosphide epitaxy on zirconium diboride

Balabalaji Padavala, H. Al Atabi, Lina Tengdelius, Jun Lu, Hans Högberg and J. H. Edgar

The self-archived postprint version of this journal article is available at Linköping University Institutional Repository (DiVA):

<http://urn.kb.se/resolve?urn=urn:nbn:se:liu:diva-144241>

N.B.: When citing this work, cite the original publication.

Padavala, B., Al Atabi, H., Tengdelius, L., Lu, J., Högberg, H., Edgar, J. H., (2018), Cubic boron phosphide epitaxy on zirconium diboride, *Journal of Crystal Growth*, 483, 115-120.

<https://doi.org/10.1016/j.jcrysgro.2017.11.014>

Original publication available at:

<https://doi.org/10.1016/j.jcrysgro.2017.11.014>

Copyright: Elsevier

<http://www.elsevier.com/>



# Cubic Boron Phosphide Epitaxy on Zirconium Diboride

Balabalaji Padavala<sup>1</sup>, H. Al Atabi<sup>1</sup>, Lina Tengdelius<sup>2</sup>, Jun Lu<sup>2</sup>, Hans Högberg<sup>2</sup> and J.H. Edgar<sup>1</sup>

Kansas State University, Department of Chemical Engineering, Durland Hall, Manhattan, KS 66506,  
USA

Thin Film Physics Division, Department of Physics, Chemistry, and Biology (IFM), Linköping  
University, SE-581 83 Linköping, Sweden

## Abstract

Cubic boron phosphide (BP) is one of the least studied III-V compound semiconductors, in part because it is difficult to prepare in high quality form. In this study, zirconium diboride ( $ZrB_2$ ) was studied as a potential substrate for BP epitaxial layers, because of its advantages of a low lattice constant mismatch and high thermal stability. Two types of substrates were considered:  $ZrB_2(0001)$  epitaxial films on 4H-SiC(0001) and bulk  $ZrB_2(0001)$  single crystals. The optimal temperature for epitaxy on these substrates was 1100 °C; higher and lower temperatures resulted in polycrystalline films. The BP film/ $ZrB_2$  interface was abrupt as confirmed by cross-sectional transmission electron microscopy, attesting to the stability of  $ZrB_2$  under BP deposition conditions. The BP films were under compressive and tensile strain on  $ZrB_2$  and  $ZrB_2/4H-SiC$  substrates, respectively, as determined by Raman spectroscopy, due to differences in the substrate/film coefficients of thermal expansion. This study suggests that with further optimization,  $ZrB_2$  can be an excellent substrate for BP epitaxial films.

## Keywords

A1. Crystal Morphology; A1. Defects; A1. Substrates; A3. Chemical vapor deposition processes; B2. Semiconducting III-V materials

## Introduction

There are two binary boron-phosphorus compound semiconductors, boron monophosphide (BP) also known as cubic boron phosphide [1-3], and boron subphosphide (denoted as  $B_{12}P_2$  or  $B_6P$ ) also known as icosahedral boron phosphide [1,4]. Both semiconductors are potentially suitable for solid state neutron detectors [5,6], due to the large thermal neutron capture cross-section of the boron-10 isotope (3855 barns) [7]. Here we focus on the epitaxial growth of BP, an indirect bandgap semiconductor ( $E_g = 2.0$  eV) [3,8]. Its distinguishing properties include an ability to exhibit both *n*- and *p*-type conductivity [3,9], a high thermal conductivity (up to  $665 \text{ W}\cdot\text{m}^{-1}\cdot\text{K}^{-1}$ ) [10,11], and a high hardness (34 GPa) [12]. Besides neutron detectors, it is also under consideration as a photocatalyst for hydrogen evolution [13] and spacers for extreme ultraviolet reflective optics [14].

Single crystal thin films are necessary for many BP device applications, and they can be prepared by chemical vapor deposition (CVD). The best single crystal substrate for BP epitaxy is unclear. Silicon has been a common substrate, but it suffers a large lattice constant mismatch (+20%) and results in high silicon concentrations ( $10^{19} \text{ cm}^{-3}$ ) in the BP film at deposition temperatures of 1000 °C or higher, presumably due to diffusion and autodoping [9]. Silicon carbide is a better substrate, due to its smaller lattice constant mismatch (-4.0%), and greater thermal stability in comparison to silicon. First used by Chu *et al* [15] in 1971, there have been several recent studies of BP epitaxy on 6H-SiC, 4H-SiC and 3C-SiC [16-18]. As a substrate, silicon carbide does have the potential disadvantage of autodoping the BP

with silicon and/or carbon. Aluminum nitride, in the form of epitaxial layers on sapphire, has also proved to be a suitable substrate for BP [19]. Its advantages include an even smaller lattice constant mismatch (-3.0%) than SiC, and a larger coefficient of thermal expansion than BP, which results in compressively stressed films, lowering the tendency for the BP films to crack, which they do under tensile stress when deposited on Si and SiC.

Here we consider zirconium diboride ( $ZrB_2$ ) as a substrate for BP epitaxy due to its high thermal stability and small lattice constant mismatch with BP (-1.3%). The coefficients of thermal expansion of  $ZrB_2$  and BP are roughly  $6 \times 10^{-6}$  to  $7 \times 10^{-6} \text{ K}^{-1}$  from 300 K to 1000 K [20] and roughly  $3.0 \times 10^{-6}$  to  $5.4 \times 10^{-6} \text{ K}^{-1}$  from 300 K to 1000 K [21], respectively. It also shares boron as an element common to both the film and the substrate. It is a refractory material with a hexagonal crystal structure ( $AlB_2$  type structure) formed by layers of boron atoms in honeycombed, graphite-like sheets, stacked between hexagonal close packed layers of zirconium. With a high melting point (3230 °C) [22],  $ZrB_2$  should be stable under all practical deposition temperatures and hence noncontaminating. It has a high electrical conductivity ( $7.0 \cdot 10^{-6} \Omega \cdot \text{cm}$ ) [23] due to its metallic bonding and electron transfer from the metal to boron sheet. This is advantageous for vertical devices, as it minimizes the electrical resistance of the substrate. It is available as epitaxial layers on Si, SiC, and  $Al_2O_3$  [24-26] and bulk crystals [27-29]. All these properties make it a potentially suitable substrate for growing BP films. Here,  $ZrB_2(0001)$  buffer layers on 4H-SiC and bulk  $ZrB_2(0001)$  crystals were tested as substrates for BP epitaxy.

### Experimental Methods and Conditions

The  $ZrB_2(0001)$  films on 4H-SiC(0001) employed in this study were prepared by high temperature direct current magnetron sputtering as developed by Tengdelius *et al* [24-26]. Briefly, this consisted of sputtering from a  $ZrB_2$  target onto a 4H-SiC(0001) substrate heated to 900 °C. The bulk  $ZrB_2(0001)$  substrates were diced and polished from a bulk crystal that was grown by a float zone technique by Otani *et al* [27].

The BP CVD reactor and sample preparation procedure were previously described by Padavala *et al* in a study of BP epitaxy on 3C-SiC [18] and AlN/sapphire [19] substrates. Most BP films were grown on ~400 nm  $ZrB_2(0001)$  buffer layers deposited on a 407  $\mu\text{m}$  thick 4H-SiC(0001) wafer; a few were deposited on ~390  $\mu\text{m}$  thick bulk  $ZrB_2(0001)$ . Substrate areas were 0.5  $\text{cm}^2$  to 1.0  $\text{cm}^2$ . The temperature of the substrates was calibrated against the thermocouple readout by melting a silicon substrate on the susceptor under actual reaction conditions. The deposition temperature mentioned throughout this paper, deduced from the thermocouple readout, is expected to closely approximate the surface temperature of the substrates. Substrates were heated to 1200 °C under  $H_2$  flow for 15 min to clean the surface prior to BP deposition. After this *in-situ*  $H_2$  etching, the temperature was reduced and stabilized at the deposition temperature (1000-1200 °C). After achieving stable temperature,  $PH_3$  was first introduced into the carrier gas stream and flowed throughout the deposition process. The deposition time starts and ends with the introduction and stoppage of  $B_2H_6$  flow. After the deposition, the temperature is slowly brought down to room temperature.  $PH_3$  is flowed during the cooling period until a substrate temperature of 800 °C. This is to prevent BP decomposition by maintaining enough phosphorus vapor pressure. All BP films discussed in this paper were deposited for 30 min. Thicknesses were not measured, but are expected to be between 1-3  $\mu\text{m}$  over the temperature range 1000-1200 °C, if the present growth rates were similar to those measured in our previous studies [17-19]. The  $H_2$  carrier gas flow rate was maintained constant at 4,000

sccm in all runs. The  $\text{PH}_3$  and  $\text{B}_2\text{H}_6$  flow rates at 1000-1100 °C were maintained at 40 sccm and 0.2 sccm, respectively. At 1200 °C, the  $\text{PH}_3$  and  $\text{B}_2\text{H}_6$  flow rates were maintained at 80 sccm and 0.4 sccm, respectively, based on the best results obtained in our previous studies [17,19]. In the present study, the  $\text{PH}_3$  and  $\text{B}_2\text{H}_6$  flow rates (or ratios) at each temperature were not varied due to the limited number of  $\text{ZrB}_2$  substrates available.

The properties of the BP/ $\text{ZrB}_2$  films were assessed in several ways. The morphology and grain size of films were imaged by optical microscopy and field emission scanning electron microscopy (FEI Nova NanoSEM 230). The orientation of the BP films, whether they were single or polycrystalline, and if other phases were present, were determined by X-ray diffraction (XRD, Rigaku Miniflex II) with a  $\text{CuK}\alpha_1$  (1.54 Å) source. Strain in the films and the crystal quality were also evaluated via Raman spectroscopy using a 0.55 m spectrometer (iHR550, Horiba/Jobin Yvon) coupled to an upright microscope (Olympus BX41) and a 633 nm HeNe laser. Whether the films contained BP and/or  $\text{B}_{12}\text{P}_2$  was determined by Raman spectroscopy and XRD. Transmission electron microscopy (TEM) cross-sectional specimens were prepared by gluing two pieces of the samples face-to-face, polishing from both sides of the specimen down to 60 µm in thickness, and finally  $\text{Ar}^-$  ion milling to electron transparency. TEM imaging was carried out by using a FEI Tecnai G2 TF20 UT high-resolution TEM instrument with a field emission gun operated at 200 kV and a point resolution of 1.9 Å.

## Results and Discussion

### Growth and Morphology of BP Films

SEM micrographs of the BP films deposited on both types of  $\text{ZrB}_2$  substrates at 1000 to 1200 °C are shown in **Figure 1**. The growth temperature had a strong effect on the morphology and crystalline orientation of BP. On both types of substrates, at 1000 °C, the films had polycrystalline features such as irregular shaped facets. These films resemble the polycrystalline BP films grown at 1000 °C on AlN [19], 4H-SiC [17] and 3C-SiC [18] substrates in our previous studies. Films deposited at 1100 °C had much better crystalline orientation with triangular BP(111) features. The average grain size increased from 0.5 µm to 2.5 µm as the temperature was increased from 1000 °C to 1100 °C. There was no evidence of  $\text{B}_{12}\text{P}_2$  formation on either type of substrate at this temperature.

At the highest deposition temperature (1200 °C), the films were a mixture of rough, randomly faceted crystallites, relatively smooth regions, and scattered icosahedrons, the latter suggesting the presence of  $\text{B}_{12}\text{P}_2$ . XRD and Raman spectroscopy analysis of these films confirmed the presence of  $\text{B}_{12}\text{P}_2$ , as discussed in subsequent paragraphs. The rough regions and  $\text{B}_{12}\text{P}_2$  formation are contrary to the results for BP deposited on AlN [19] and 4H-SiC [17] substrates at 1200 °C under same deposition conditions; there the BP films were highly ordered and free of  $\text{B}_{12}\text{P}_2$ . The reason  $\text{B}_{12}\text{P}_2$  forms on  $\text{ZrB}_2$  substrates but not on the other substrates at a deposition temperature of 1200 °C is unknown.

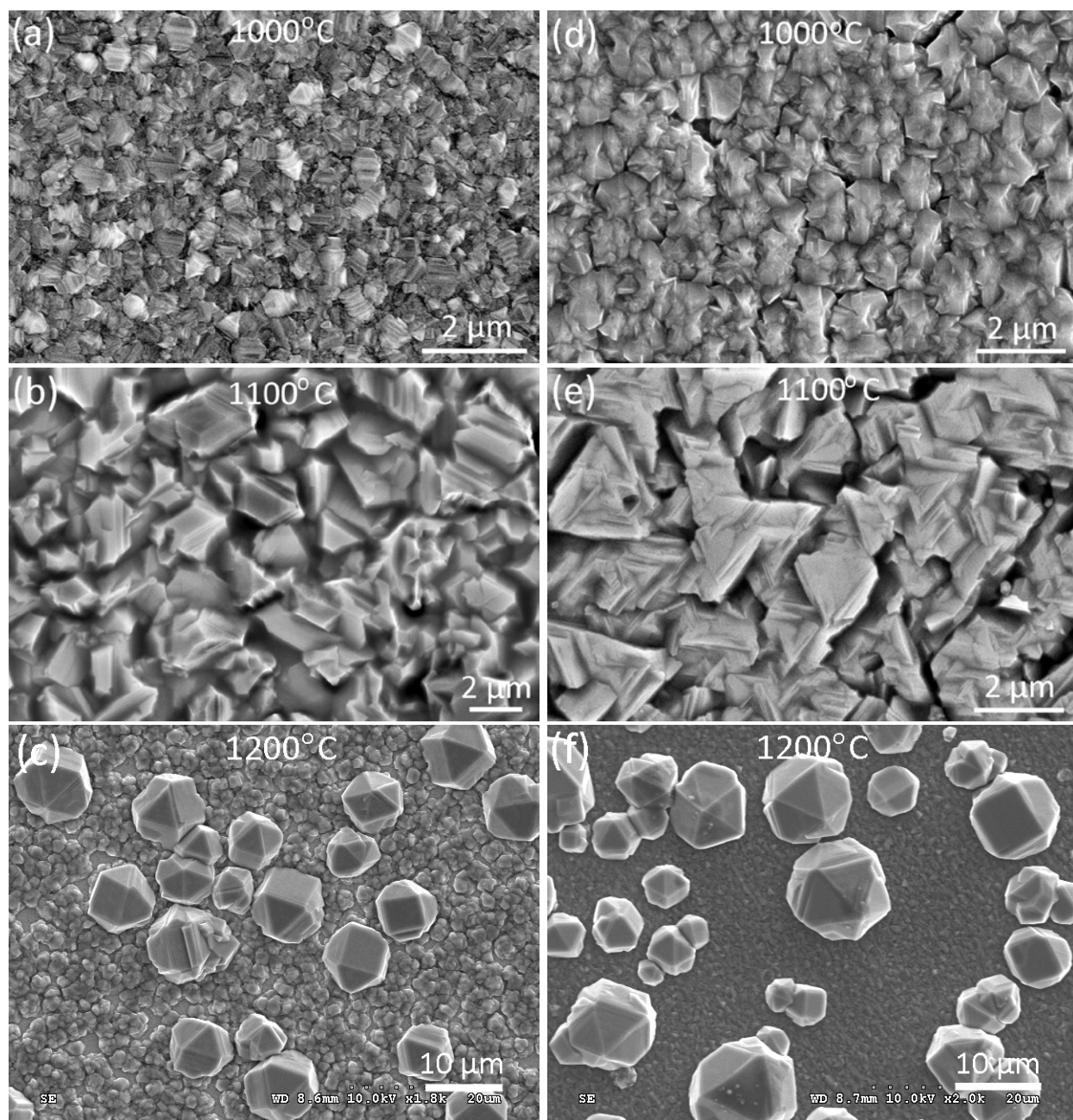


**Figure 1. Morphology of BP films deposited on (a,b,c) ZrB<sub>2</sub>/4H-SiC and (d,e,f) bulk ZrB<sub>2</sub> at different temperatures.**

A low-magnification cross-section TEM of the BP film grown on the 400 nm thick ZrB<sub>2</sub> layer on 4H-SiC substrate at 1100 °C revealed the presence of defects in the BP layer (**Figure 2a**). The highest density of defects was closest to the BP/ZrB<sub>2</sub> interface, and decreased toward the free surface. Faceting of the BP film was evident. The BP film on bulk ZrB<sub>2</sub> was similar (**Figure 2b**).

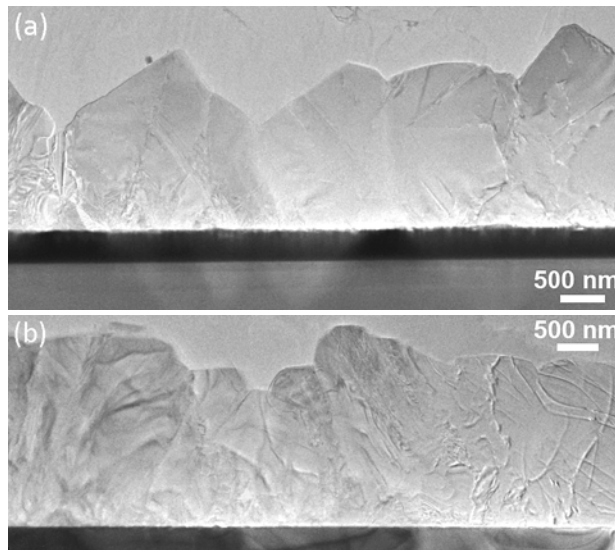


**Figure 2.** Cross sectional TEM overview of the BP layer deposited on (a)  $\text{ZrB}_2/4\text{H-SiC}$  and (b) bulk  $\text{ZrB}_2$  at 1100 °C.

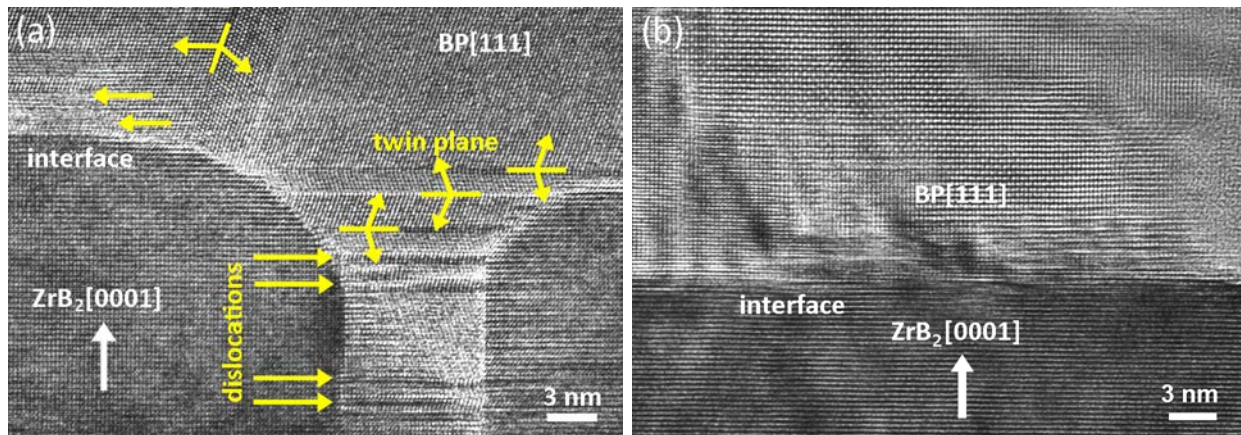


**Figure 3.** High resolution TEM images depicting defects at the BP- $\text{ZrB}_2$  interface for films grown at 1000 °C on (a)  $\text{ZrB}_2/4\text{H-SiC}$  and (b) bulk  $\text{ZrB}_2$ .

Higher resolution TEM images of the BP interface with  $\text{ZrB}_2/4\text{H-SiC}$  and bulk  $\text{ZrB}_2$  substrates for films grown at 1100 °C are shown in **Figure 3**. Epitaxial growth was achieved on both substrates. There were many stacking faults and dislocations in the BP films near the interface. The interface was smoother for the BP film on  $\text{ZrB}_2/4\text{H-SiC}$  substrate compared to the bulk  $\text{ZrB}_2$  substrate; still there were plenty of twin boundaries on the {111} planes, stacking faults, and dislocations in the BP. These twin planes (shown in **Figure 3a**) indicate the rotational twinning in BP films. Rotational twinning typically happens when there is a mismatch in crystal symmetry between the epilayer and underlying substrate. In the present case, BP has a zinc blende crystal structure and the underlying  $\text{ZrB}_2$  and 4H-SiC substrates have hexagonal crystal structure. The preferred orientation of BP(111) on  $\text{ZrB}_2(0001)$  has a 3-fold symmetry while the hexagonal  $\text{ZrB}_2(0001)$  has a 6-fold symmetry. Due to this difference in crystal symmetry, the BP(111) film deposits in two different orientations, rotated by 180° with respect to each other. A deep pit was seen at the interface in **Figure 3a**, indicating the  $\text{ZrB}_2$  film was not uniformly deposited on 4H-SiC prior to the BP deposition. This may be a consequence of the microstructure of  $\text{ZrB}_2$  films on SiC [24]. It is possible

that grains boundaries are etched faster by the H<sub>2</sub> introduced prior to the deposition of the BP. In summary, there were BP(111) twins on ZrB<sub>2</sub> substrates due to the difference in symmetry between BP(111) and ZrB<sub>2</sub>(0001).

### Crystalline Orientation of BP

The XRD patterns recorded for the BP films grown on ZrB<sub>2</sub>/4H-SiC substrates at three temperatures are shown in **Figure 4**. The diffraction patterns for 1000 °C and 1100 °C showed no significant difference between the two, although SEM micrographs indicated polycrystalline and crystalline films at 1000 °C and 1100 °C, respectively. The presence of B<sub>12</sub>P<sub>2</sub> in the BP film deposited at 1200 °C was evident from XRD pattern. Multiple peaks associated with B<sub>12</sub>P<sub>2</sub> were present at several two-theta angles, including 22° and 46°, representing the (012) and (024) planes, respectively. In addition, a few minor peaks from unwanted orientations of ZrB<sub>2</sub> formed during its deposition on 4H-SiC were identified.

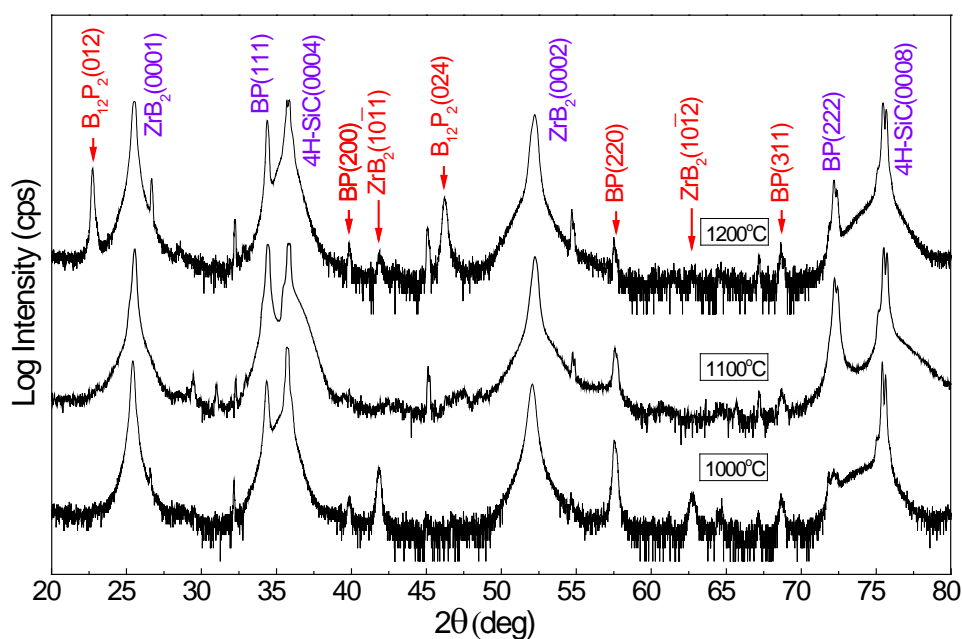


**Figure 4. XRD patterns of BP films deposited on ZrB<sub>2</sub>(0001)/4H-SiC at different temperatures.**

The FWHM of preferred BP(111) orientation, and peak intensity ratios of BP(111) with other undesired orientations of BP such as (200) and (220) were measured from XRD  $\theta$ - $2\theta$  scans as shown in **Figures 5a** and **b**. The peak width of BP(111) increased with temperature from 1000 °C to 1100 °C, then decreased as the temperature was further increased to 1200 °C, to a value lower than the value at 1000 °C. The intensity ratios followed a similar trend (see **Figure 5b**) with change in temperature. These plots indicate the evolution of polycrystalline growth of BP and decreased crystal quality at both 1000 °C and 1200 °C.

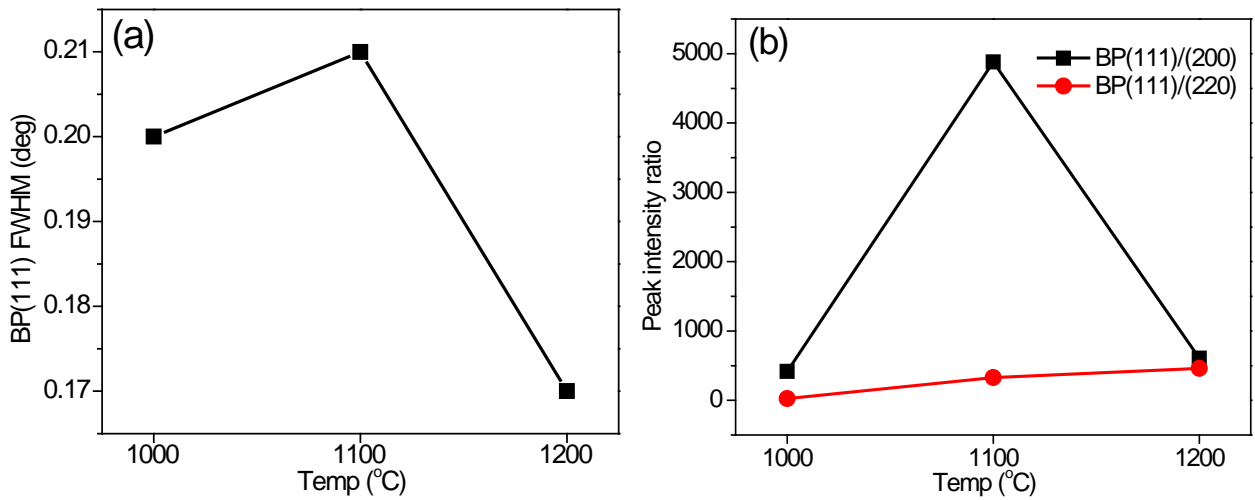


**Figure 5. (a) FWHM of BP(111) and (b) peak intensity ratios measured from XRD  $\theta/2\theta$  scans on  $\text{ZrB}_2/4\text{H-SiC}$  substrate.**

The Raman spectra of BP films deposited on  $\text{ZrB}_2/4\text{H-SiC}$  and bulk  $\text{ZrB}_2$  in the temperature range 1000-1200 °C are shown in **Figure 6**. The measured BP Raman peaks were consistent with the reported values in the literature [30]: i.e. a strong LO phonon peak is located at approximately  $829\text{ cm}^{-1}$ . The peak at  $\sim 475\text{ cm}^{-1}$  confirms that  $\text{B}_{12}\text{P}_2$  was also deposited at 1200 °C on both types of substrates. This peak at  $\sim 475\text{ cm}^{-1}$  is typically the most intense Raman peak for  $\text{B}_{12}\text{P}_2$ . Based on the SEM, XRD and Raman spectroscopy results presented above, we conclude that the best temperature to deposit a crystalline BP on  $\text{ZrB}_2$  was 1100 °C.

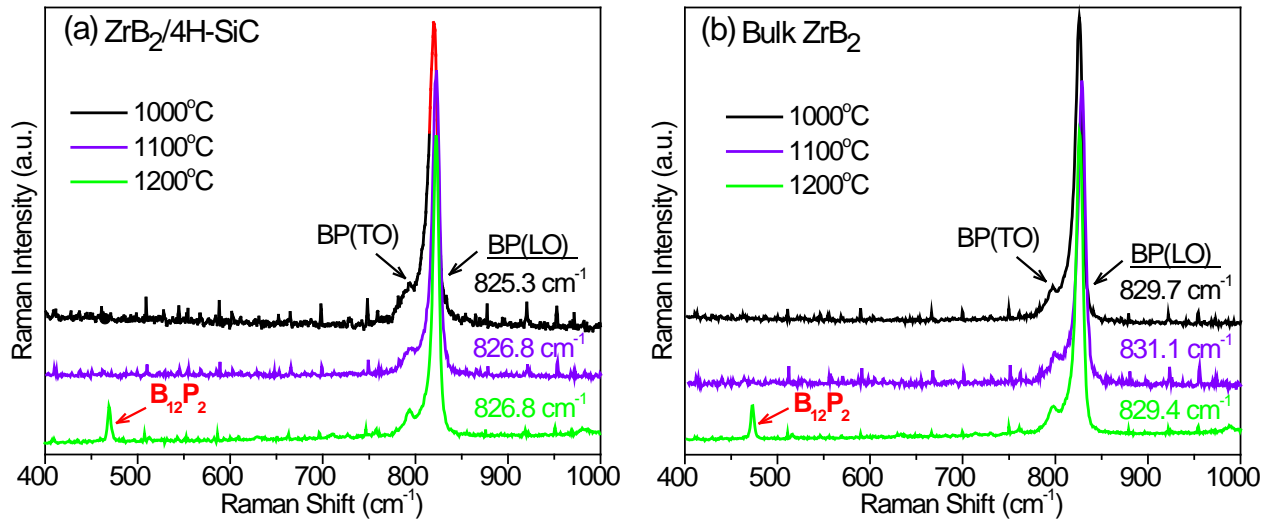


**Figure 6. Raman spectra depicting the peak positions of BP(LO) mode on (a)  $\text{ZrB}_2/4\text{H-SiC}$  and (b) bulk  $\text{ZrB}_2$  at different temperatures.**

The FWHMs of BP(LO) Raman peak and peak position on both substrates were measured and tabulated in **Table 1**. The Raman peak FWHM consistently decreased with increasing temperature, in agreement with the results reported for BP on Si, 4H-SiC [17], and AlN/sapphire [19] substrates. A consistent difference in the BP(LO) peak position was evident between the two substrates at a given temperature as shown in **Table 1**.

**Table 1. Comparison of BP(LO) peak's FWHM and position for films on bulk ZrB<sub>2</sub> and ZrB<sub>2</sub>/4H-SiC**

Temp (°C)	FWHM (cm <sup>-1</sup> )		Position (cm <sup>-1</sup> )	
	ZrB <sub>2</sub> /4H-SiC	Bulk ZrB <sub>2</sub>	ZrB <sub>2</sub> /4H-SiC	Bulk ZrB <sub>2</sub>
1000	11.9	10.1	825.3	829.7
1100	9.7	9.4	826.8	831.1
1200	7.7	8.4	826.8	829.4

**Figure 7** shows the comparison of BP(LO) peak position between the two substrates at 1100 °C along with the peak position of relatively strain-free BP whiskers grown on 4H-SiC(0001) via VLS mechanism. For growth on bulk ZrB<sub>2</sub>, the BP(LO) peak is at higher energy than the BP(LO) of BP whiskers [18], the opposite being true for growth on ZrB<sub>2</sub>/4H-SiC.

This trend is largely due to the differences in thermal expansion between ZrB<sub>2</sub>/4H-SiC and bulk ZrB<sub>2</sub> substrates. The thermal expansion of ZrB<sub>2</sub> is roughly between  $6 \times 10^{-6}$  to  $7 \times 10^{-6}$  K<sup>-1</sup> from 300 K to 1000 K [20] whereas that of BP it is between  $3.0 \times 10^{-6}$  to  $5.4 \times 10^{-6}$  K<sup>-1</sup> from 300 K to 1000 K [21]. Under compression, the BP peak position shifts to higher wavenumbers [31]. Under tension, it shifts to lower wavenumbers. In the case of BP on bulk ZrB<sub>2</sub>, the films experience compressive strain due to the larger coefficient of thermal expansion of ZrB<sub>2</sub> compared to BP, resulting in the higher peak position. In the case of ZrB<sub>2</sub>/4H-SiC, although the thin ZrB<sub>2</sub> layer has a higher coefficient of thermal expansion than BP, the overall thermal expansion is dominated by the much thicker 4H-SiC substrate. As reported earlier, BP films experience tensile strain on 4H-SiC, resulting in the shift of BP(LO) to lower wavenumbers [17]. Hence the peak position for BP on ZrB<sub>2</sub>/4H-SiC was shifted to the lower side, due to the tensile strain, consistent with earlier findings.

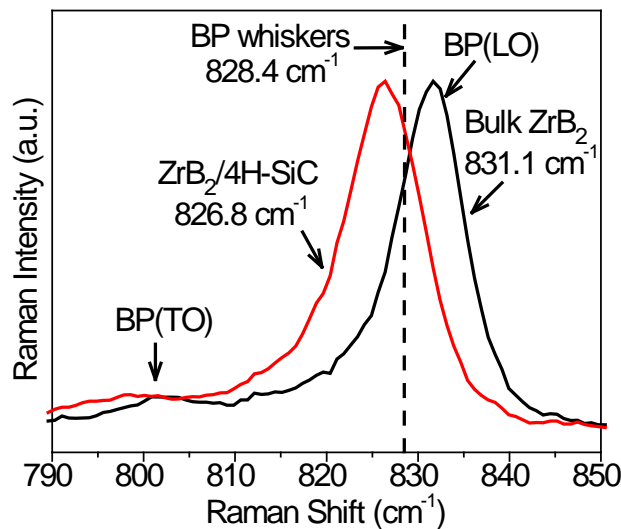


**Figure 7. Comparison of the BP(LO) mode position on ZrB<sub>2</sub>/4H-SiC and on bulk ZrB<sub>2</sub> at 1100 °C.**

On the other hand, comparing the peak position of BP(LO) mode for BP growth on the two substrates as mentioned in **Table 1**, the band shifted to higher wavenumbers by 1.4-1.5 cm<sup>-1</sup> when the growth temperature increased from 1000 °C to 1100 °C. But when the temperature was further increased

to 1200 °C the BP peak position did not change for BP on ZrB<sub>2</sub>/4H-SiC while it decreased on the bulk ZrB<sub>2</sub> substrate. The direction the peak shifts with increasing temperature was expected to be opposite for both substrates based on their coefficients of thermal expansion (as explained in the previous paragraph) as well as our past findings [17,19]. Thus, a clear trend in shift of peak position was not evident with change in deposition temperature for both substrates. Based on these findings, we conclude that the overall shift in peak position with change in temperature could be largely attributed to the difference in thermal expansion coefficients between BP and underlying substrate, however, contributions from the strain fields from defects, differences in the substrate surface structure, and the properties of the BP film could also be significant.

## Conclusions

This study shows that BP epitaxy is possible on both bulk ZrB<sub>2</sub>(0001) and ZrB<sub>2</sub>(0001)/4H-SiC substrates. Temperature is one important parameter for controlling the crystallinity of the BP films. A lower temperature (1000 °C) resulted in polycrystalline BP while the higher temperature (1200 °C) resulted in both polycrystalline BP and formation of B<sub>12</sub>P<sub>2</sub>. The optimum temperature for depositing epitaxial BP in this study was 1100 °C. Transmission electron microscopy confirmed the BP/ZrB<sub>2</sub> interface was abrupt; diffusion between the materials was negligible. Given the inherent advantages of ZrB<sub>2</sub> as a substrate for BP, additional studies are worthwhile.

## Acknowledgements

This research was supported by the Department of Energy grant number GEGF001846. LT acknowledges support from the Swedish Research Council (VR), contract 621-2010-3921. JL and HH acknowledge financial support from the Swedish Government Strategic Research Area in Materials Science on Functional Materials at Linköping University (Faculty Grant SFO-Mat-LiU No.2009-00971). The bulk zirconium diboride crystal provided by Hiroshi Amano which were grown by Shigeki Otani, NIMS, are greatly appreciated.

## References

- [1] F.V. Williams, R.A. Ruehrwein, The preparation and properties of boron phosphides and arsenides, *J. Am. Chem. Soc.* 82 (1960) 1330-1332.
- [2] B. Stone, D. Hill, Semiconducting properties of cubic boron phosphide, *Phys. Rev. Lett.* 4 (1960) 282-284.
- [3] R.J. Archer, R.Y. Koyama, E.E. Loebner, R.C. Lucas, Optical absorption, electroluminescence, and the band gap of BP, *Phys. Rev. Lett.* 12 (1964) 538-540.
- [4] R.A. Burmeister, Jr., P.E. Greene, Synthesis and crystal growth of B<sub>6</sub>P, *Trans. Metal. Soc. AIME* 239 (1967) 408-13.
- [5] J.C. Lund, F. Olschner, F. Ahmed, K.S. Shah, Boron phosphide on silicon for radiation detectors, *Mater. Res. Soc. Symp. Proc.* 162 (1990) 601-604.

- [6] T.P. Viles, B.A. Brunett, H. Yoon, J.C. Lund, H. Hermon D. Buchenauer. K. McCarty, M. Clifft, D. Dibble, R.B. James, Material requirements for a boron phosphide thermal neutron counter, Mater. Res. Soc. Symp. Proc. 487 (1998) 585-590.
- [7] J.W. Meadows, J.F. Whalen, Thermal-neutron-absorption cross sections of Li-6 and B-10, Nucl. Sci. Eng. 40 (1970) 12-16.
- [8] J. I. Ejembi, I. H. Nwigboji, L. Franklin, Y. Malozovsky, G. L. Zhao, D. Bagayoko, Ab-initio calculations of electronic, transport, and structural properties of boron phosphide, J. Appl. Phys. 116 (2014) 103711.
- [9] Y. Kumashiro, Refractory semiconductor of boron phosphide, J. Mater. Res. 5 (1990) 2933–2947.
- [10] G.A. Slack, Nonmetallic crystals with high thermal conductivity, J. Phys. Chem. Solids 34 (1973) 321-335.
- [11] L. Lindsay, D.A. Broido, T.L. Reinecke, First-principles determination of ultrahigh thermal conductivity of boron arsenide: a competitor for diamond, Phys. Rev. Lett. 111 (2013) 025901.
- [12] D.G. Clerc, Mechanical hardness: atomic-level calculations for diamond-like materials, J. Mater. Sci. Lett. 17 (1998) 1461-1462.
- [13] L. Shi, P. Li, W. Zhou. T. Wang, K. Chang, H. Zhang, T. Kako, G. Liu, J. Ye, n-type boron phosphide as a highly stable, metal-free, visible-light active photocatalyst for hydrogen evolution 28 (2016) 158-163.
- [14] V.V. Medvedev, A.E. Yakshin, R.W.E. van de Kruijs, F. Bijkerk, Phosphorus-based compounds for EUV multilayer optics materials, Optical Mater. Express 5 (2015) 1450-1459.
- [15] T.L. Chu, J.M. Jackson, A.E. Hyslop, S.C. Chu, Crystals and epitaxial layers of boron phosphide, J. Appl. Phys. 42 (1971) 420–424.
- [16] G. Li, J.K.C. Abbott, J.D. Brasfield, P. Liu, A. Dale, G. Duscher, P.D. Rack, C.S. Feigerle, Structure characterization and strain relief analysis in CVD growth of boron phosphide on silicon carbide, Appl. Surf. Sci. 327 (2015) 7-12.
- [17] B. Padavala, C. Frye, Z. Ding, R. Chen, M. Dudley, B. Raghathamachar, N. Khan, J.H. Edgar, Preparation, properties and characterization of boron phosphide films grown on 4H- and 6H-silicon carbide, Solid State Sci. 47 (2015) 55-60.
- [18] B. Padavala, C.D.Frye, X. Wang, B. Raghathamachar, J.H. Edgar, CVD growth and properties of boron phosphide on 3C-SiC, J. Cryst. Growth, 449 (2016) 15-21.
- [19] B. Padavala, C.D. Frye, X. Wang, Z. Ding, R. Chen, M. Dudley, et al., Epitaxy of Boron Phosphide on Aluminum Nitride(0001)/Sapphire Substrate, Cryst. Growth Des. 16 (2016) 981–987.
- [20] N.L. Okamoto, M. Kusakari, K. Tanaka, H. Inui, S. Otani, Anisotropic elastic constants and thermal expansivities in monocrystal CrB<sub>2</sub>, TiB<sub>2</sub>, and ZrB<sub>2</sub>, Acta Materialia 58 (2010) 76-84.
- [21] G.A. Slack, S.F. Bartram, Thermal expansion of some diamond-like crystals, J. Appl. Phys. 46 (1975) 89-98.

- [22] K.I. Portnoi, L.G. Romashov, L.N. Burobina, Phase diagram of the zirconium-boron system, *Sov. Powder Met. Met. Ceram.* 7 (1970) 68.
- [23] H.J. Juretschke, R. Steinitz, Hall effect and electrical conductivity of transition-metal diborides, *Phys. Chem. Solids* 4 (1958) 118-127.
- [24] L. Tengdelius, J. Birch, J. Lu, L. Hultman, U. Forsberg, E. Janzén, H. Högberg, Magnetron sputtering of epitaxial  $ZrB_2$  thin films on 4H-SiC(0001) and Si(111), *Phys. Stat. Solidi A* 211 (2014) 636-640.
- [25] L. Tengdelius, G. Greczynski, M. Chubarov, J. Lu, U. Forsberg, L. Hultman, E. Janzén, H. Högberg, Stoichiometric, epitaxial  $ZrB_2$  thin films with low oxygen-content deposited by magnetron sputtering from a compound target: Effects of deposition temperature and sputtering power, *J. Crystal. Growth* 430 (2015) 55-62.
- [26] L. Tengdelius, E. Broitman, J. Lu, F. Eriksson, J. Birch, T. Nyberg, L. Hultman, H. Högberg, Hard and elastic epitaxial  $ZrB_2$  thin films on  $Al_2O_3$ (0001) substrates deposited by magnetron sputtering from a  $ZrB_2$  compound target, *Acta Materialia*, 111 (2016) 166-172.
- [27] S. Otani, M.N. Korsukova, T. Mitsuhashi, Preparation of  $HfB_2$  and  $ZrB_2$  single crystals by the floating-zone method, *J. Cryst. Growth* 186 (1998) 582-586.
- [28] H. Kinoshita, S. Otani, S. Kamiyama, H. Amano, I. Akasaki, J. Suda, H. Matsunami,  $ZrB_2$  substrate for nitride semiconductors, *Jpn. J. Appl. Phys. Pt. 1* 42 (2003) 2260-2264.
- [29] H. Kinoshita, S. Otani, S. Kamiyama, H. Amano, I. Akasaki, J. Suda, H. Matsunami, Zirconium diboride (0001) as an electrically conductive lattice-matched substrate for gallium nitride, *Jpn. J. Appl. Phys.* 40 (2001) L1280L1282.
- [30] O. Brafman, G. Lengyel, S.S. Mitra, P.J. Gielisse, J.N. Plendl, L. C. Mansur, Raman spectra of aluminum nitride, cubic boron nitride, and boron phosphide, *Solid State Communications* 6 (1968) 523-526.
- [31] J.A. Sanjurjo, E. López-Cruz, P. Vogl, M. Cardona, Dependence on volume of the phonon frequencies and their effective charges of several III-V semiconductors, *Phys. Rev. B* 28 (1983) 4579-4584.